Lawrence Livermore Laboratory

STATISTICAL MECHANICS OF REACTING DENSE PLASMAS

F. J. Rogers

November 22, 1978

This paper was prepared for submission to

Conference on Dense Plasmas, Pasadena, CA, November 14-16, 1978

STATISTICAL MECHANICS OF REACTING DENSE PLASMAS*

F. J. Rogers
University of California Lawrence Livermore Laboratory
Livermore, California 94550

Abstract

A review of the quantum statistical theory of strongly coupled many component plasmas is given. The theoretical development is shown to consist of six separate parts. Compensation between bound and scattering state contributions to the partition function and use of the shifted Debye energy levels are important aspects of the analysis. The results are valid when the electrons are moderately coupled to the heavy ions, i.e. $\Lambda^*_{e\alpha} < 1$, but no restriction is placed on the coupling between heavy ions. Another restriction is that $\lambda/\lambda_D < 1$, i.e., the thermal deBroglie wavelength is less than the Debye length. Numerical calculations of $PV/N_0 kT$ and C_V are given for a Rubidium plasma.

I. Introduction

The equation of state of plasmas has been an active research area for many years. During most of this time interest has been stimulated by astrophysical applications. Besides being directly applicable to such problems as predicting the evolutionary history of stars, the state of ionization and equation of state, are also required in opacity and transport calculations. Additionally, very good equation of state calculations will be required to adequately answer the current question concerning the conditions for which multi-component plasmas phase separate.[1] In recent years interest in the properties of partially ionized matter has been stimulated by laser fusion, MHD, and other energy generation research programs.

Early research was based on analogy with dissociative equilibrium in molecular gases which have an ideal limit for very low densities. This met with immediate difficulties since ionic and atomic partition functions are non-convergent. Various ad hoc methods for cutting off the divergence were introduced. The first successful calculation of non-ideal effects was made in 1923 by Debye and Huckel, whose interest was in electrolytic solutions. Subsequent workers added the Debye-Huckel free energy to the ideal plasma model free energy. The ionization state and thermo-properties were then obtained by free energy minimization. A summary and exhaustive list of references of work prior to 1966 is given by Brush.[2] A good review and list of references up through 1975 is given in the monograph by Ebeling, Kraeft and Kremp.[3]

Due to the analytical complexity of a rigorous treatment of non-ideal plasmas most of the literature cited in the above review articles is concerned with hydrogen plasmas.[2] These results are very important to our fundamental

understanding but have limited applications. Besides being restricted to $Z=1$, they are also limited to low density. Two recent attempts to treat slightly non-ideal plasmas for arbitrary Z and all stages of ionization have been given.[4,5] These are based on free energy minimization procedures which require some assertions as to how individual atoms and ions can be uncoupled from the plasma. In the present paper we avoid making these assertions by working in the grand canonical formalism or what Krasnikov[3] calls the "physical model". Furthermore high Z plasmas for which the ions are very non-ideal, while the electrons are moderately non ideal will be treated.

II. Outline of Theoretical Method

Most of what will be discussed in this article has been published elsewhere.[6,7] The objective here is to summarize the theory and identify the most salient points. Some of the theory concerning strongly coupled ions and calculations of the equation of state of Rubidium are new.

Figure 1 is a flow chart of the theoretical method. Step 1 introduces the Mayer S-function which is a sum over all cluster integrals or alternatively the virial coefficients. Since the neglect of the uncertainty principle causes the electron-ion terms to diverge as $r \to 0$. It is obvious at the outset that reacting plasmas require quantum mechanics. This type of divergence only involves few body terms. A more intransigent type of divergence occurs in all virial and cluster coefficients for Coulomb systems in the limit $r \to \infty$. This divergence is essentially classical and can only be removed through many-body summation procedures. Each contribution to the many body sum has only small quantum modifications for $r < \chi$, the thermal de Broglie wavelength. As a result it is possible to carry out the many-body

analysis classically and insert Slater sums at the appropriate places in the final result in order to remove the few-body electron-ion divergencies. The result is rigorous provided the ratio χ/λ_D is <1. Correction terms in χ/λ_D can be added at a later stage of the analysis.

In step 2 we follow the work of Abe[8] who showed for the one-component plasma model (OCP) that the long range divergencies can be eliminated by appropriate reorganizations in powers of the potential (βU). The leading term in the resultant expression for S is the familiar Debye-Huckel Correction. Higher order terms resemble virial coefficients for the screened Coulomb potential. Since we are interested in real many component plasmas it is necessary to carry out a multi-component generalization of Abe's work. After the appropriate introduction of quantum mechanics this yields the equation of state of non-ideal completely ionized gases according to

$$(F-F_0)/VkT = -S \tag{1}$$

$$\frac{P}{kT} = \sum_i \rho_i + S - \sum_i \rho_i \frac{\partial S}{\partial \rho_i} \tag{2}$$

In order to use Eqs. (1-2) to calculate the equation of state for incomplete ionization it is necessary to make assertions as to how composite particles enter the ideal gas free energy, F_0, and the S function. The resulting expressions can then be used to minimize the free energy with respect to changes in the composition.

Since ionization equilibrium is naturally included in the grand canonical formalism it is the fundamentally correct way to treat this aspect of the problem. Unfortunately it is subject to all the divergencies present in the canonical formalism and other more complicated divergencies as well. In step

3 a procedure for avoiding this difficulty is introduced. This is to find a method for generating the activity expansion as a functional of S, thereby obtaining a divergence free expression for P/kT in the grand canonical formalism. Degeneracy corrections are added to the leading terms of this expression using the method of Cooper and DeWitt.[9] Some additional remarks concerning this step are given in Appendix A.

The S function involves virial coefficients for the Debye potential. In order to properly treat ionization equilibrium it is necessary to collect all the bound state terms that contribute to each power of the activity and thus obtain the cluster coefficients for the Debye potential, e.g., $z^3 b_3 = z^3(-B_3/2 + 2/B_2^2)$. This corresponds to step 4 of Figure 1. In Figure 4 some specific examples for the second and third cluster coefficients are given. The underlined numeral subscripts indicate multicomponent structure.

The procedure for incorporating composite particles into the activity equations, rests on the observation that the formation of bound states for $kT < E_b$, the binding energy, lowers the order of the cluster coefficients. For example, due to its exponential temperature dependence the bound state part of the electron-ion second cluster coefficient, $b_{e\alpha}$, enters the cluster expansion like a new ideal particle, while the continuum state part enters like a real two-body interaction between electrons and ions. Because of this it is necessary to introduce an augmented set of activity variables, such that, the leading term in the revised activity series corresponds to the Saha ionization equilibrium equation.[6,7] Scattering states only appear in the interaction corrections of the properly ordered activity series, i.e., proper treatment of bound clusters requires the decomposition of the trace into bound and scattering parts. This corresponds to the first part of step 5 in Figure 1.

The renormalization of the grand partition function, just described, works with the complete trace, so that, some latitude in how one defines a composite particle is afforded. An improper decomposition will ultimately be rectified through high order terms. However, since in general only a few low order terms will be evaluated, a physically realistic decomposition must be made. It has been shown that the well known compensation between bound and scattering states leads naturally to a proper decomposition procedure.[7] The resulting effective bound state sum is convergent and there is no need to invoke any cutoff criteria as was done in early work on this problem. A specific example of how the two body cluster term is split is shown in Figure 5. In brief it shows the two leading terms in the bound state high temperature expansion included with the scattering state contribution. This is because as shown in Ref. 7 (1977) these terms almost precisely cancel similar terms in the scattering state part of the trace.

At this point we have shown how to identify composite particle contributions in the S expansion, but only in the ideal gas limit. To go beyond this we need to reorganize the terms so that those terms that correspond to composite particles enter the interaction corrections similar to fundamental particles; e.g., the Debye length must be transformed according to $\lambda_D(z_e + Z^2 z_\alpha) \rightarrow \lambda_D(z_e + Z^2 z_\alpha + (Z-1)^2 z_{e\alpha} + \dots)$. The first step in this process is indicated in Figure 6. An explicit expression for the activity of one-electron composites appears on Figure 7. Since $\Lambda_{e\alpha}^*$ depends on the activity according to $z^{1/2}$, terms in the expansion of exp $(\Lambda_{e\alpha}^*)$ go together with similar terms in Λ_{ii}^* appearing elsewhere in the S expansion and give rise to the transformation of the Debye length indicated above. An important result of this, as shown in Figure 7, is that the energy levels that enter the definition of $z_{e\alpha}$ are the shifted Debye

energy levels. Due to the expansion in terms of Λ^*_{ij} the resulting equations, as a practical matter, are only applicable when $\Lambda^*_{ij} < 1$.

Since when $Z \gg 1$

$$\Lambda^*_{\alpha\alpha} = \frac{z^2 e^2}{kT\lambda_D} > 1$$

for most interesting regions of ρ, T space, the methods being discussed here will for practical purposes be limited to $Z < 4$; unless some way to incorporate strong ion coupling is introduced.

The final step in Figure 1 is therefore to go beyond the perturbation expansion for the classical ion-ion contribution. This is accomplished by considering the complete set of ion terms, i.e., $s_{\alpha\alpha}$, $s_{\alpha\alpha\alpha}$, etc. as a group. By performing accurate numerical calculations for $s_{\alpha\alpha}$ and $s_{\alpha\alpha\alpha}$ a general fitting formula for all the $s_{\underline{n}}$ is extracted. When $z^2 z_\alpha / z_e \gg 1$ it follows that $S_{ion} \rightarrow S_{OCP}$ so that we can check the reliability of the fitting function. It is found to be very good for $\Gamma = (\Lambda^2/3)^{1/3} < 10$. An additional correction factor is then applied to bring the fit results into agreement with the OCP in the high Z limit.

When $Z \gg 1$ the S expansion can be shown to inadequately treat the heavy ion contribution and it is necessary to recollect terms so that the most important term from each group of terms involving S a sequentially larger number of times must be added to get the leading non-ideality correction. Next all the second most important terms must be added, etc. The final result of this is

$$\frac{P}{kT} = z_e + z_\alpha + z_{e\alpha} + \ldots + P_1 + P_2 + \ldots \tag{4}$$

where

$$P_1 = S + \sum_i z_i (e^{\frac{\partial S}{\partial z_i}} - 1 - \frac{\partial S}{\partial z_i}) \tag{5}$$

$$P_2 = \frac{1}{2} \sum_{ij} z_i z_j \frac{\partial S}{\partial z_i \partial z_j} (e^{\frac{\partial S}{\partial z_i}} - 1)(e^{\frac{\partial S}{\partial z_j}} - 1) \tag{6}$$

$$S = S_{ion} + z_e e^2/kT \lambda_D + z_e^2 s_{ee} + 2z_e z_\alpha s_{e\alpha}^c + 2z_e z_{e\alpha} s_{e,e\alpha}^c + \ldots \tag{7}$$

$$S_{ion} = z_\alpha z^2 e^2/kT \lambda_D + s_{\alpha\alpha} + s_{\alpha\alpha\alpha} + \ldots \tag{8}$$

III.   Numerical Calculations

A.   Energy Levels and Phase Shifts

To evaluate thermodynamic properties of strongly coupled reacting plasmas using the results of Section II requires a large computer code which is referred to as ACTEX.   In order to calculate composite particle activities we need to obtain multi-electron energy levels for the Debye potential. Calculation of multiparticle scattering states is also required.   This will be accomplished through the introduction of effective-two particle potentials, e.g., the interaction of an electron with Rb^+ is treated as a two-body problem.   The potential used to calcuate energy levels is shown in Figure 8. It is composed of a long range part and exponential screened Coulomb terms for each shell of core electrons.   The parameters in the potential are determined by solving a relativistic wave equation such that it reproduces the ground state energies of experimentally measured members of a given isoelectronic

sequence. The functions α, β, γ, etc. were then obtained by a least squares fit. Excited states having the same parentage as the ground state can also be calculated with the $V(Z,r)$ given in Figure 8. To calculate the energy of states of different parentage one could obtain slightly different functions α, β, γ for each distinct parent state. Since this would be a large undertaking, all states having a parentage different from the ground state are added by finding fitting functions that locate their positions relative to the states of the $V(Z,r)$ potential. These states are obtained by solving the wave equation for particular values of Z.

The procedure just described yields accurate energy levels for multi-electron bound states in the isolated ion limit. What is actually required are the energy levels for the Debye potential. These are obtained by adding a Debye screening factor to the long range part of the potential. This is clearly valid when λ_D >> than the core radius. By solving a two-electron variational problem it can be shown that the screening of only the long-range part of $V(Z,r)$ yields quite good results except when the binding energy of the outermost electrons approaches zero. This can be seen in Figure 9 where one and two parameter variational calculations for He are compared with solutions to the Schroedinger equation using the potential $V(Z,r)$.

The potential $V(Z,r)$ can also be used to calcuate the continuum contribution for electron-composite ion interactions. If the charge distribution is considered rigid one can use electrostatics to transform $V(Z,r)$ into an ion-ion potential. This is shown at the bottom of Figure 9 for H_e^+-H_e^+ interactions.

B. The Equation of State

To obtain the equation of state it is necessary to iterate Eqs. 4-8 until the density constraints of Figure 2 are satisfied. Rubidium has been chosen to illustrate the nature of the results that are obtained. Figure 10 gives the approximate range of ρ, T space for which the condition $\Lambda^*_{e\alpha} < 0.8$ is satisfied. The curve for $\tilde{x}/\lambda_D < 1$ lies well inside the shaded region. The peculiar shape of this region is due to the fact that for fixed density the Coulomb coupling increases with decreasing temperature. For densities somewhat less than normal solid density the low temperature state is a neutral gas so that the Coulomb coupling falls back to zero and the equations are subject to the convergence properties of ordinary gases. The lower branch of the shaded region has not actually been located and is intended only to be schematic. For the alkali metals it is possible to make calculations below the lower limit branch by assuming that the fundamental species are electrons and Rb^+ ions whose cores are uncoupled from the plasma.

Figure 11 gives ACTEX calculations of $PV/N_0 kT$ vs T for densities of 0.0001, 0.1, 1.0 and 10.0 g/cc corresponding to the solid lines. Also plotted except for 0.1 g/cc are some Thomas-Fermi-Kirzhnits (TFK) calculations[12] with OCP ion corrections. Shell structure effects are very prominent in the low density ACTEX results. Due to the large energy difference, as the temperature is reduced, there is a large separation between the filling of the K-shell and the onset of L-shell formation. The separation between the L and M shells is much less and only a change in slope is observed between the M and N shells. There is again a large separation between the filling of the 4p subshell and the formation of neutral 5s Rb atoms. The TFK results are found to be a remarkably good average of the quantum statistical curve. The maximum

differences are approximately 10% when T > 100 eV and around 30% in the 1 < T < 5 range.

The ACTEX results for ρ = 0.1 g/cc show a considerable lessening of the shell structure effects although the K-L shell separation is still large. For ρ = 1.0 g/cc the L-M shell separation is observable only as a change in slope. At this density the TFK results differ from the ACTEX results by at most 9% when T > 100 eV. At ρ = 10 g/cc the ACTEX calculations shows only slight shell structure effects even for the K shell. The difference between the two calculations at this density is no more than 4% when T > 200 eV. Even though the percentage errors are small the TFK calculations grossly misrepresents the non-ideality correction in the kilovolt range where the plasma is almost completely ionized. Correspondingly, the percentage errors for low Z plasmas are somewhat higher than those found here for Rb.

Figure 12 shows ACTEX for various orders of approximation. The curve labeled Saha corresponds to turning off all interaction terms, i.e. retaining only the activity terms of order z. The curve labeled 5/2 expansion includes all interaction terms through 5/2 powers in the activity. The curve labeled OCP ion-ion correction corresponds to Eqs. 4-8 and the curve labeled N* is the corresponding total number of free particles, i.e. the total number of free electrons plus one. The 5/2 expansion curve is seen to differ at most by 7% with the Saha curve, whereas, using ion-ion corrections fitted to the OCP result produces results which differ by as much as 19%. The ion correction is actually somewhat larger than this indicates since the ionization state has now been shifted up to the N* curve. In fact the ion correction reduces the pressure by 38% at T = 100 eV.

Figure 13 gives C_V/38 k vs T obtained from ACTEX for various densities. The curves show considerable structure and density dependence. In the

temperature range plotted there are three main peaks for $\rho = 0.0001$ g/cc. The one around 1200 eV corresponds to the filling of the K-shell. The one around 280 eV corresponds to the L-shell, and the structured peak around 70 eV corresponds to the filling of the 4s and 4p subshells. It is not plotted but the TFK curve is in error by more than a factor of two and shows no shell structure effects. The specific heat curves are considerably smoothed as the density is increased but still show appreciable shell structure oscillations at 10 g/cc.

From the results presented here it is clear that the TFK theory yields good equation of state results in a smoothly averaged way. They are even good quantitatively for the pressure but are of little value, except at high densities for any application which depends on derivative quantities such as sound speed and specific heat.

IV. Concluding Remarks

This paper has reviewed the theoretical apparatus for going beyond intuitive model approaches for obtaining the equation of state of strongly coupled reacting plasmas. By concentrating on the underlying analytic structure, rather than a diagrammatic study of various orders of approximation, it has been possible to derive an activity expression which simultaneously treats ionization equilibrium and strong ion coupling. This work should have many applications in applied problems of current interest. The results presented here are representative of the type of data that can be generated. It is anticipated that in the future this work will be extended so that the restriction on $\Lambda_{e\alpha}^{*}$ can be relaxed and that the general approach will be extended to include non-equilibrium properties.

Some possible topics for future work, depending on interest, are:

1) Calculate high order electron-ion terms using the pseudopotential method presented in Ref. 7 (1978). This is of particular importance to singly ionized alkali plasmas.

2) Study transport coefficients to see if compensation between bound and scattering states, and the introduction to the shifted Debye energy levels has any fundamental impact.

3) Evaluate computationally fast model approaches in common use and make modifications to bring them into closer agreement with fundamentally correct approach.

4) Invert the activity expression to find the best free energy minimization procedure.

5) Continue the isoelectronic energy level fitting procedure to higher Z sequences.

6) Extend diffraction and exchange corrections.

7) Carry out analysis for two temperature plasmas such that electrons and ions equilibrate among themselves but not each other.

Appendix A

S-Expansion for Multi-Component Quantum Plasmas

In step 3 we are essentially treating a completely ionized quantum system of electrons and nuclei. No hint of composite particles has yet entered the analysis. Therefore the activity expression at this point need only be a function of z_e and z_i, the activities of electrons and nuclei respectively. The resulting expression is shown in Figure 2. To the terms given P/kT appears to be a simple extension of the corresponding one component result given in Figure 1. However, cross derivatives start to appear in the next group of terms beyond those given which considerably complicate the analysis.

Figure 3 displays the leading terms in the S-function. It is shown that the leading term is just the Debye-Huckel term. Corrections in $\bar{\lambda}/\lambda_D$ to this term have been given by DeWitt[10] and also Rogers[7] (1978). The s_{ij} are the negative of the virial coefficients except the lowest two orders of perturbation in $(\beta\xi_i\xi_j)$ are subtracted out. When $\bar{\lambda}/\lambda_D \approx 1$ the second order term needs to be modified.[6] For quantum systems the two-body virial coefficient can be calculated from the Beth-Uhlenbeck expression where the $E_{n\ell}(\lambda_D)$ are the energy levels for the screened Coulomb potential. These are modified to some extent when $\bar{\lambda}/\lambda_D \approx 1$. The δ_ℓ are the corresponding phase shifts, and p is the relative momentum. For heavy ions the classical virial coefficient is always adequate. For B_{ee} some modifications of the Beth-Uhlenbeck formula to account for exchange are necessary.[11]

References

1. E. L. Pollack and B. J. Alder, Phys. Rev. $\underline{A15}$, 1263 (1977), D. J. Stevenson, Phys. Rev. $\underline{B12}$, 3999 (1975).

2. Stephen G. Brush, "Progress in High Temperature Physics and Chemistry" edited by C. A. Rouse, Vol. 1, 1 (1967).

3. W. Ebeling, W. D. Kraeft, D. Kremp, "Theory of Bound States and Ionization Equilibrium in Plasmas and Solids", Akademie-Verlag (Berlin, 1977).

4. W. Ebeling, Physica $\underline{73}$, 573 (1974).

5. Yu. G. Krasnikov and V. I. Kucherenko, Teplofiz. Vys. Temp. $\underline{16}$, 43 (1978).

6. F. J. Rogers and H. E. DeWitt, Phys. Rev. $\underline{A8}$, 1061 (1973).

7. F. J. Rogers, Phys. Rev. $\underline{A10}$, 2441 (1974), Phys. Lett. $\underline{61A}$, 358 (1977), LLL Report UCRL-80933 (1978).

8. R. Abe, Prog. Theor. Phys. (Kyoto) $\underline{22}$, 213 (1960).

9. M. S. Cooper and H. E. DeWitt, Phys. Rev. $\underline{A8}$, 1910 (1973).

10. H. E. DeWitt, J. Math. Phys. $\underline{3}$, 1216 (1962); J. Nucl. Energy $\underline{C2}$, 27 (1961).

11. F. J. Rogers, Phys. Rev. $\underline{A4}$, 1145 (1971).

12. S. L. McCarthy, "The Kirzhnits Corrections to the Thomas Fermi Equation of State", UCRL-14363 (1965).

Mayer virial expansion

$$S = \sum_{i=2} \eta^i \beta_{i,1} / J$$

$$= \sum_{j=2} \eta^j B_j / J - 1$$

where η = Density

β_{j-1} = Cluster integral

B_j = Virial coefficient

(1)

Abe reorganizations in powers of βu

$$S = S_{ring} + \sum_{j=2}^{\sim} S_j \, (T, \eta, \lambda_D)$$

where $S_{ring} = 1/12 \, \pi \, \lambda_D^3$ and the S_j resemble virial coefficients for the Debye potential.

(2)

a) Find procedure for generating the activity series from

$$S(T, z, \lambda_D)$$

i.e., $\dfrac{P}{kT} = z + S + \sum_{m=2}^{\infty} \left(\dfrac{\partial}{\partial z} z\right)^{m-2} \left(\dfrac{\partial S}{\partial z}\right)^m / m!$

b) Add degeneracy

(3)

Collect terms in S-expansion in terms of powers of z, i.e., introduce cluster coefficients for the Debye potential,

$$\beta u_s = \xi_i \, \xi_j \, e^{-r/\lambda_D} / r,$$

and insert Slater sums

(4)

Introduce augmented set of activity variables. Recollect term on basis of effective n-body interactions.

Valid for $\Lambda_{ij}^{*} = \dfrac{\xi_i \, \xi_j}{kT \lambda_D} \simeq 1$

$\gamma = \dfrac{\lambda}{\lambda_D} < 0.5$

(5)

Renormalize equations to account for strong ion coupling.

Valid for Λ_{ee}^{*}, $\Lambda_{ei} \simeq 1$

Λ_{ii}^{*} arbitrary, $\gamma < 0.5$

(6)

Thermal properties of plasmas at all stages of ionization

(7)

Fig. 1. Schematic of theoretical procedure

Mayer S-function

$$S(z_e, z_\alpha) = - \sum_{\underline{J}=2}^{\infty} B_{\underline{J}} \, z^{\underline{J}} / (\underline{J}-1)$$

Activity of species i

$$z_i = (2s + 1) \, \lambda^{-3} e^{\mu_i / kT}$$

Two-component S-expansion

$$\frac{P}{kT} = z_e + z_\alpha + S + \frac{z_e}{2!} \left(\frac{\partial S}{\partial z_e}\right)^2 + \frac{z_\alpha}{2!} \left(\frac{\partial S}{\partial z_\alpha}\right)^2 + \ldots$$

Parametric density relations

$$n_e = z_e \, \frac{\partial (P/kT)}{\partial z_e} \, , \, n_\alpha = z_\alpha \, \frac{\partial (P/kT)}{\partial z_\alpha}$$

Fig. 2. P/kT as a functional of S

$$S(z_e, z_\alpha) = S_R + z_e^2\, s_{ee} + 2z_e z_\alpha s_{e\alpha} + z_\alpha^2 s_{\alpha\alpha} + z_e^3 s_{eee} + \dots$$

Debye-Hückel correction

$$S_R = 1/(12\pi\lambda_D^3)\,,\ \lambda_D = \left\{ kT/[4\pi e^2 (z_e + \sum_i Z_i^2 z_i)] \right\}^{1/2}$$

$$s_{ij} = - B_{ij}(\lambda_D) + 2\pi\lambda_D^2 \left(\frac{\xi_i \xi_j}{kT}\right) - \frac{\pi}{2}\left(\frac{\xi_i \xi_j}{kT}\right)^2 \lambda_D$$

Beth-Uhlenbeck virial coefficient

$$B_{ij} = - \sqrt{2}\,\lambda_{ij}^3 \left(\sum_{n\ell} (2\ell + 1)\, e^{-\beta E_{n\ell}^{(\lambda_D)}} \right.$$

$$\left. + \frac{1}{\pi} \sum_{\ell} (2\ell + 1) \int_0^\infty dp\, \frac{d\delta_\ell}{dp} e^{-p^2/2\mu_{ij}kT} \right)$$

Fig. 3. Cont.) two-component S-expansion

$$C_{\underline{2}} \equiv S_{\underline{2}} = z_e^2\, s_{ee} + 2z_e z_\alpha s_{e\alpha} + z_\alpha^2 s_{\alpha\alpha}$$

$$C_{\underline{3}} \equiv S_{\underline{3}} + \frac{z_e}{2!}\left(\frac{\partial S_2}{\partial z_e}\right)^2 + \frac{z_\alpha}{2!}\left(\frac{\partial S_2}{\partial z_\alpha}\right)^2$$

$$C_{\underline{n}} \to z^{\underline{n}}\, b_{\underline{n}} \text{ as } \lambda_D \to \infty$$

Fig. 4. Cluster coefficients for the plasma pot.

E. G. split the two body trace

$$S_{e\alpha} = S_{e\alpha}^b + S_{e\alpha}^c$$

where

$$S_{e\alpha}^b = z_e z_\alpha \sqrt{2}\, \lambda_{e\alpha}^3 \sum_{n\ell} (2\ell + 1)\, (e^{-E_{n\ell}/kT} - 1 + E_{n\ell}/kT)$$

$$S_{e\alpha}^c = z_e z_\alpha \frac{\sqrt{2}\lambda_{e\alpha}^3}{\pi} \int_0^\infty \left(\sum_\ell (2\ell + 1)\, dp \frac{d\delta_\ell}{dp}\, e^{-p^2/2\mu_{e\alpha}kT} \right.$$

$$\left. + \omega_0 - \omega_1 \right) + 2\pi\lambda_D^2 \left(\frac{\xi_i \xi_j}{kT}\right) - \frac{\pi}{2}\left(\frac{\xi_i \xi_j}{kT}\right)^2 \lambda_D$$

and

$$\omega_0 \equiv \sum_{n\ell} (2\ell + 1) = \frac{8}{9\sqrt{3\pi}} (Z\lambda_D/a_0)^{3/2} - 0.2289$$

$$\omega_1 \equiv \sum_{n\ell} (2\ell + 1)\, E_{n\ell}/kT = \left(\frac{32}{15\sqrt{5\pi}} (Z\lambda_D/a_0)^{1/2} - 0.4932\right)/kT$$

Fig. 5. Introduce composite particle activities

$$S_{e\alpha}(\lambda_D) \equiv e^{\Lambda_{e\alpha}^*} z_{e\alpha}$$

where

$$\Lambda_{e\alpha}^* = \frac{Ze^2}{kT\lambda_D}$$

when $\Lambda_{e\alpha}^* < 1$, a useful expansion is

$$S_{e\alpha}(\lambda_D) = (1 + \Lambda_{e\alpha}^* + \Lambda_{e\alpha}^{*2}/2\cdots)\, z_{e\alpha}$$

Fig. 6. Define an activity for one electron composites

$$\lambda_D \longrightarrow \lambda_D^* = \left\{ kT / \left[4\pi e^2 \left(z_e + Z^2 z_\alpha + (Z-1)^2 z_{e\alpha} + \ldots \right) \right] \right\}^{1/2}$$

Composite particle activity

$$z_{e\alpha} = 2 z_e z_\alpha \left[2^{1/2} \lambda_{e\alpha}^3 \sum_{n\ell} (2\ell+1) \left(e^{-E_{n\ell}^s / kT} - \Delta \right) \right]$$

$$\Delta = (\omega_0 - \omega_1) e^{-\Lambda_{e\alpha}^*}$$

Shifted energy levels

$$E_{n\ell}^s (\lambda_D^*) = E_{n\ell} (\lambda_D^*) - Ze^2 / \lambda_D^*,$$

$$\frac{P}{kT} = z_e + z_\alpha + z_{e\alpha} + \ldots + \chi_R^* + C_{\underline{2}}^* + \ldots$$

$$\chi_R^* = S_R^* + \sum_i \frac{z_i}{2} \left(\frac{\partial S_R^*}{\partial z_i} \right)^2 + \ldots$$

Fig. 7. Cont.) $Z^{5/2}$ expansion for complex plasmas

$$V(Z, r) = \left[(Z-A) + A_K e^{-\alpha(Z-A_K+1)r} \right.$$
$$\left. + A_L e^{-\beta(Z-A_K-A_L+1)r} \ldots \right] / r$$

Where $A = A_K + A_L + \ldots = $ total number of bound electrons

$$\alpha, \beta, \gamma = \left\{ \alpha_0, \beta_0, \gamma_0 + \frac{(\alpha_1, \beta_1, \gamma_1)}{Z} + \frac{(\alpha_2, \beta_2, \gamma_2)}{Z^2} \right\},$$

Obtained by iteration, using a relativistic wave,
EQ. to match experimental data

Fitting function for states of different parentage

$$\frac{E - E_g}{E_{(\eta+1)s} - E_g} = \frac{1}{Z} \left(a_0 + \frac{a_1}{Z} + \frac{a_2}{Z} \right)$$

For the DEBYE POT: $(Z-A)/r \rightarrow (Z-A)e^{-r/\lambda_D}/r$
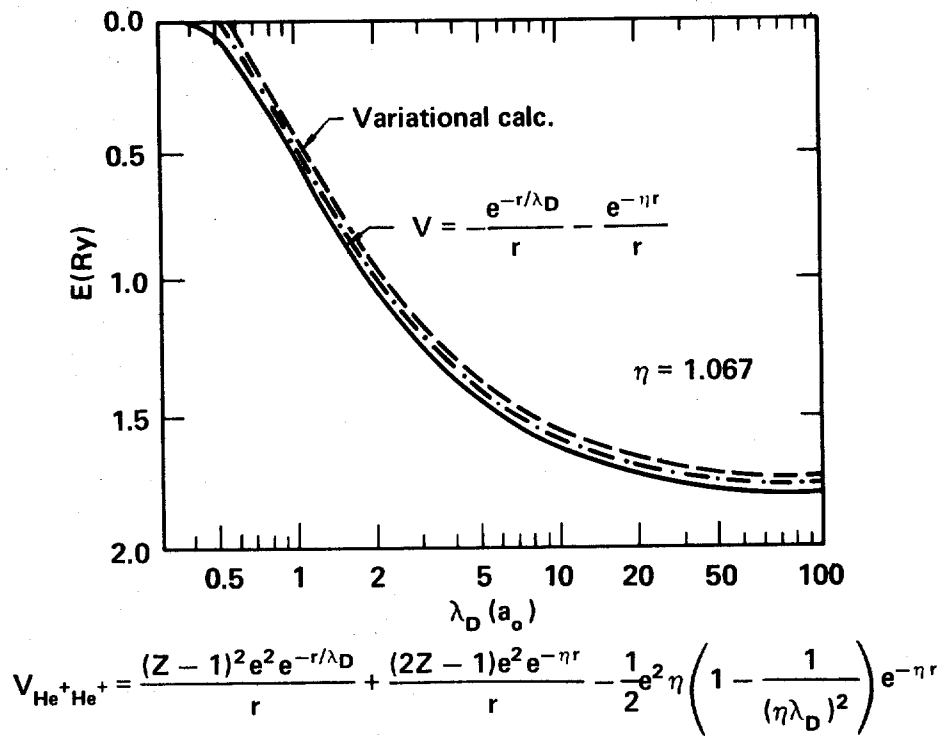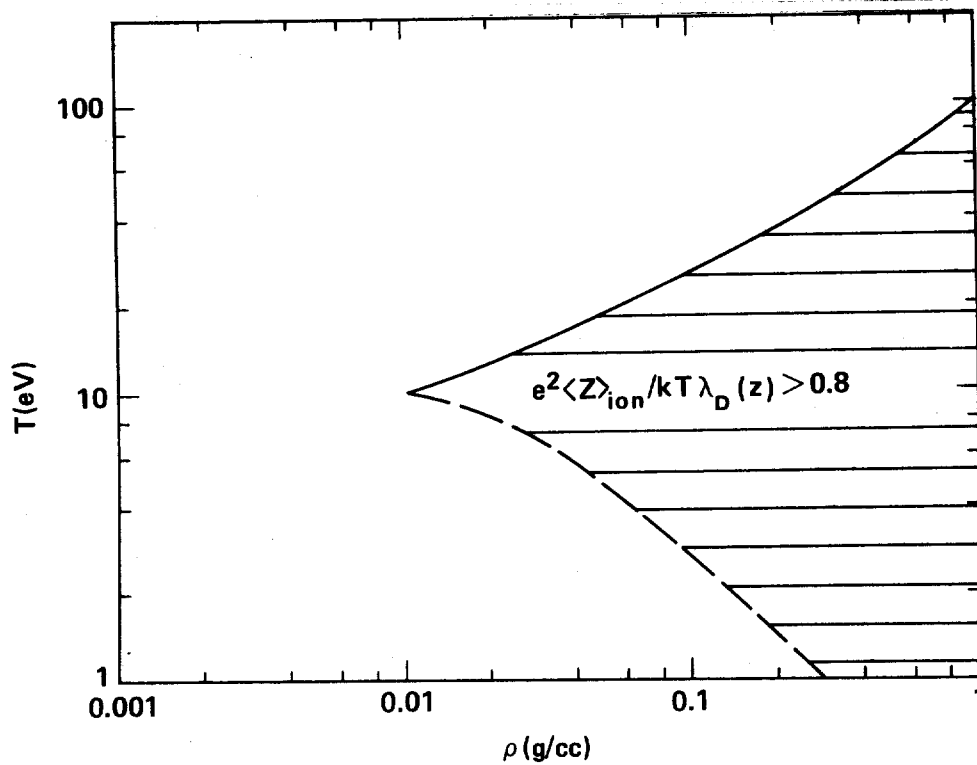
Fig. 8. Isoelectronic potential

$$V = -\frac{e^{-r/\lambda_D}}{r} - \frac{e^{-\eta r}}{r}$$

$$\eta = 1.067$$

$$V_{He^+He^+} = \frac{(Z-1)^2 e^2 e^{-r/\lambda_D}}{r} + \frac{(2Z-1)e^2 e^{-\eta r}}{r} - \frac{1}{2}e^2 \eta \left(1 - \frac{1}{(\eta\lambda_D)^2}\right)e^{-\eta r}$$

Fig. 9. Ground state energy of He vs λ_D

$$e^2 \langle Z \rangle_{ion}/kT\lambda_D(z) > 0.8$$
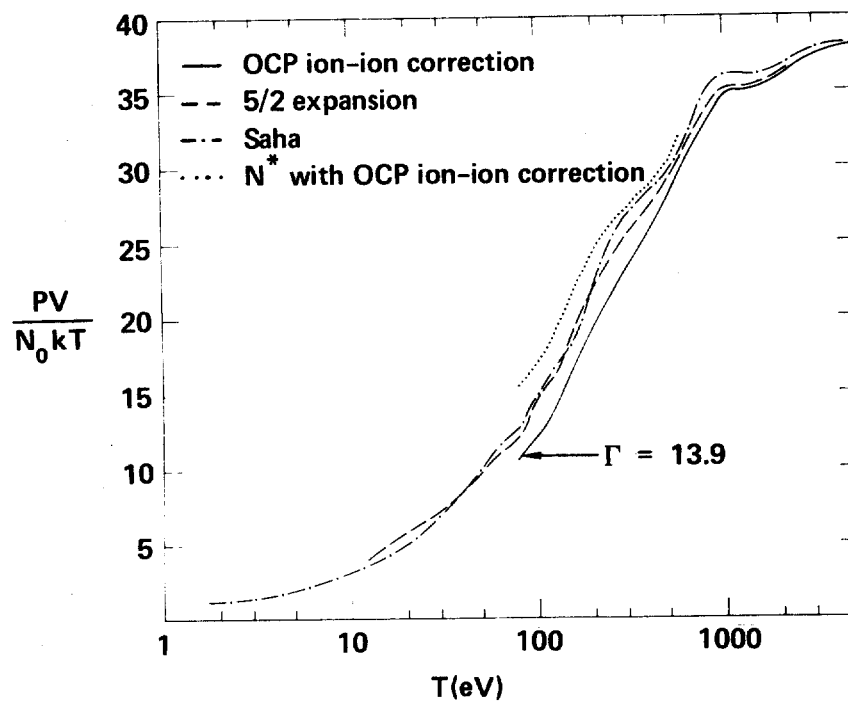
Fig. 10. Range of validity for rubidium
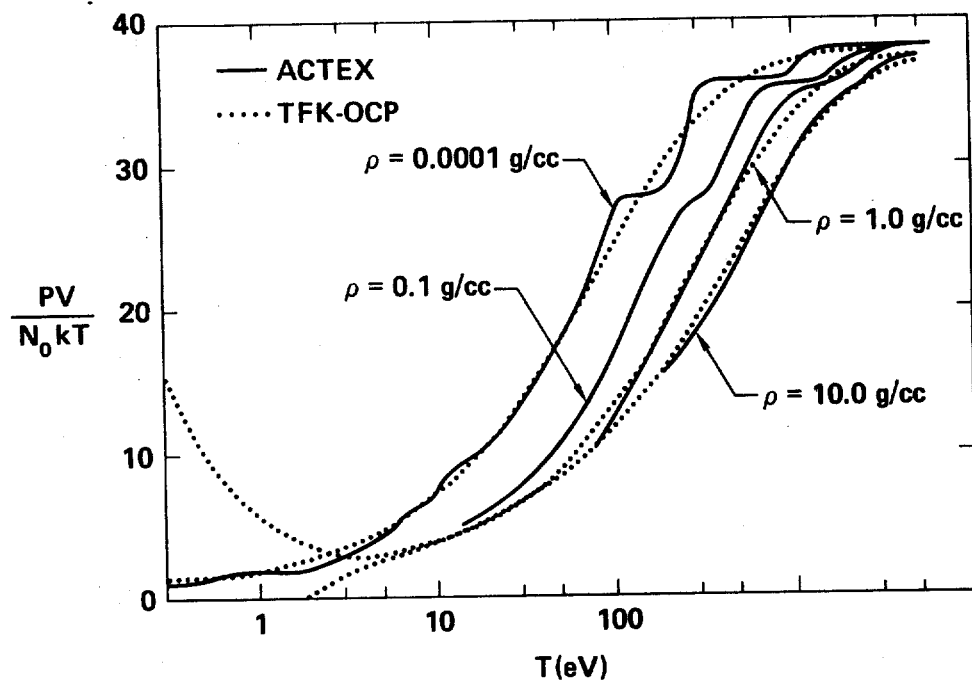
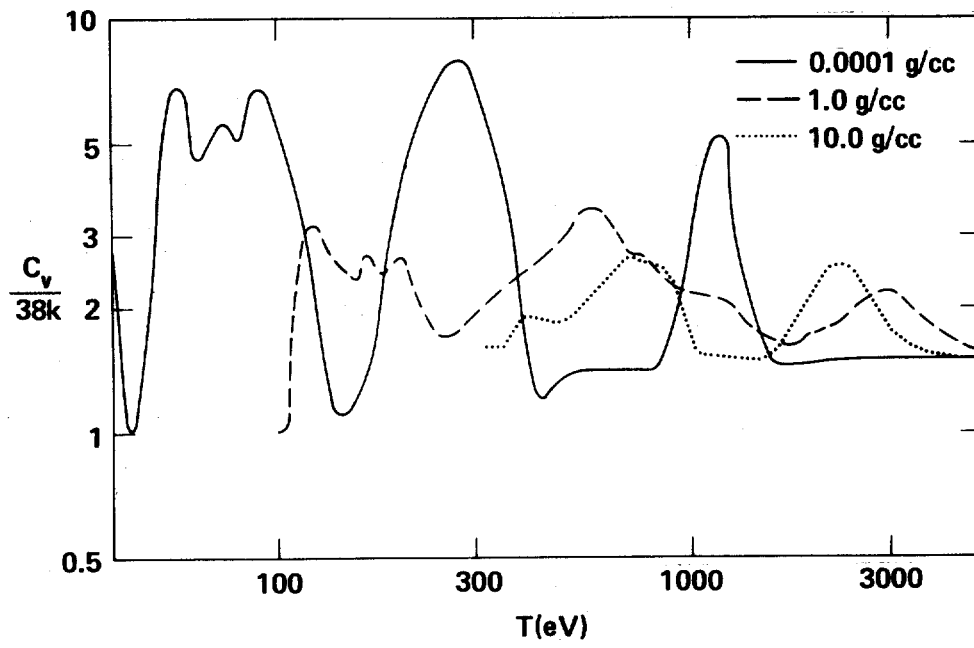Fig. 11. Rubidium: PV/No kT vs temperature

Fig. 12. Contributions to pressure for RB at 1.0 g/cc

Fig. 13. Rubidium specific heat